Resonance enhancement of electron collision rates for fluorinelike ions

K. J. Reed, M. H. Chen and A. U. Hazi
High Temperature Physics Division, University of California, Lawrence Livermore National Laboratory, Livermore, California 94550
(Received 4 May 1987)

The distorted-wave approximation and similar weak-coupling methods are frequently used to calculate electron collision cross sections for studies of astrophysical and laboratory plasmas. Autoionizing resonances neglected in these approximations can significantly enhance the calculated rates for collisional excitation of some transitions in highly charged ions. We investigated the effects of such resonances on the excitation rates for $n=2$ to $n=2$ transitions in fluorinelike Fe, Se, Mo, Ag, Xe, and Eu. The background excitation rates were calculated using a relativistic distorted-wave approximation, and the detailed Auger and radiative rates were calculated using a multiconfiguration Dirac-Fock model. The largest effect is on the electric-dipole-forbidden transitions. The enhancement diminishes with increasing atomic number for all transitions.

I. INTRODUCTION

Cross sections for electron collisional excitation of positively charged ions are important for studies of astrophysical plasmas and plasmas produced in laboratory experiments. Because reported measurements of electron-ion excitation cross sections or rate coefficients are scarce, there is heavy reliance upon calculated data[1] for use in codes which have been developed to model such plasmas. The distorted-wave approximation and similar weak-coupling methods are frequently employed to calculate[1] electron collision cross sections for highly charged ions. These methods usually provide a faster means of computing cross sections than the more accurate close-coupling methods,[1] and are very useful if cross sections are required for a large number of transitions. However, the neglect of indirect resonance contributions to the cross sections is a major limitation of these methods. It has been recognized for some time that autoionizing resonances can significantly enhance the calculated rates for electron collisional excitation of some transitions in light positive ions.[1] More recently, similar enhancements have been found in studies of highly charged ($Z^* \geq 10$) ions. For example, Pradhan *et al.*[2] found large resonance enhancement of the excitation rates for electric-dipole-forbidden transitions in heliumlike ions. Calculations using multistate close-coupling methods[3] and quantum-defect theory[4] have shown significant enhancements in Li-like ions. In studies of neon-like krypton, it was found that the $2p^5 3lnl'$ resonances increased the excitation rates for the $2p^6\,{}^1S \rightarrow 2p^5 3s\,{}^3P$ transition by a factor of 2 near threshold.[5] Similar results were reported by Pindzola *et al.*[6] for the same transition in Ti^{12+}.

We have calculated rates for electron-impact excitation of $n=2$ to $n=2$ transitions in fluorinelike ions, and we examined the effects of autoionizing resonances on these rates. Fluorinelike ions, and other ions with partially filled L shells, are important constituents of plasmas produced in magnetic fusion devices[7] and in laser-heated targets.[8,9] In particular, neonlike ions of Se, Y, and Mo have been successfully used to demonstrate lasing in the soft-x-ray regime.[9,10] Dielectronic recombination of F-like ions[11] has an important effect on the excited-state kinetics of the Ne-like soft-x-ray laser scheme.[12,13] Furthermore, theoretical models predict that during much of the lifetime of the plasma fluorinelike ions are present in abundances up to 50%, and substantial gains have been predicted[14] for some transitions in Se^{23+}.

Previously, a few calculations of non-resonant, electron-impact excitation cross sections have been reported for ions in the fluorine isoelectronic sequence. Distorted-wave cross sections for the $n=2$ to $n=3$ transitions in Fe^{17+} have been reported by Merts *et al.*[15] and rate coefficients for some of these same transitions are given by Davis *et al.*[16] A detailed study of electron collisional excitation of Se^{25+} by Hagelstein includes cross sections for all $n=2$ to $n=3$ transitions.[14] Cross sections for the $n=2$ to $n=2$ transitions in Ti^{13+} and Kr^{27+} have been reported by Bhatia *et al.*[17,18]

In this paper we report both background (non-resonant) and resonance enhanced collision rates for the three $n=2$ to $n=2$ transitions in fluorinelike Fe, Se, Mo, Ag, Xe, and Eu. A study of the Z dependence and scaling of the excitation cross sections will be given in a future publication.[19]

II. CALCULATIONAL PROCEDURE

The resonances are produced when the incoming electron excites a fluorinelike ion and is simultaneously captured, forming a doubly excited neonlike ion. The doubly excited ion may radiatively decay or autoionize. The radiative channel leads to dielectronic recombination. If autoionization occurs, the resulting fluorinelike ion may be left in an excited state, and the overall effect is a contribution to the excitation cross section.

We consider the following two-step processes:

$$2s^2 2p_{1/2}^2 2p_{3/2}^3 + e \rightarrow 2s^2 2p_{1/2} 2p_{3/2}^3 nln'l' \rightarrow 2s^2 2p_{1/2} 2p_{3/2}^4 + e \ , \quad (1a)$$

$$2s^2 2p_{1/2}^2 2p_{3/2}^3 + e \rightarrow 2s 2p_{1/2}^2 2p_{3/2}^3 n \ln' l' \rightarrow 2s 2p_{1/2}^2 2p_{3/2}^4 + e \ , \quad (1b)$$

$$2s^2 2p_{1/2} 2p_{3/2}^4 + e \rightarrow 2s 2p_{1/2} 2p_{3/2}^4 nln'l' \rightarrow 2s 2p_{1/2}^2 2p_{3/2}^4 + e \ . \quad (1c)$$

The background cross sections without resonances were calculated using a relativistic multiconfiguration distorted-wave code (MCDW) developed by Hagelstein.[20] This code is part of an atomic physics package YODA (Ref. 20) which is also used to calculate the atomic energy levels using relativistic, multiconfiguration wave functions. In the F-like target calculation, we included the ground state $2s^2 2p_{1/2}^2 2p_{3/2}^3$, the two lowest excited states $2s^2 2p_{1/2} 2p_{3/2}^4$ and $2s 2s_{1/2}^2 2p_{3/2}^4$, and also all of the numerous configurations formed by promotion of an $n=2$ electron to an $n=3$ excited state.

For the dipole-forbidden transition, [Eq. (1a)], partial waves up to $l=12$ were sufficient to converge to cross sections at all energies up to ten times threshold. For the other two transitions, which are electric dipole allowed, partial waves up to $l=70$ were computed to ensure convergence. Assuming a Maxwellian distribution for the plasma electrons at temperature T, the rate coefficient C_{ij} (in cm^3/s) for collisional excitation from initial state i to final state j is given by[1]

$$C_{ij} = \frac{8.63 \times 10^{-6}}{g_i T^{1/2}} \exp(-E_{ij}/kT) \gamma_{ij} \ . \quad (2)$$

Here E_{ij} is the transition energy and g_i is the statistical weight of the initial level. γ_{ij} is the rate parameter given by

$$\gamma_{ij} = \int_0^\infty \Omega_{ij} \exp(-E_j/kT) d(E_j/kT) \ , \quad (3)$$

where E_j is the energy of the scattered electron, and the collision strength Ω_{ij} is related to the collision cross section Q_{ij} by

$$Q_{ij} = \frac{\Omega_{ij}}{g_i E_i} \pi a_0^2 \ . \quad (4)$$

Here, a_0 is Bohr radius and E_i is the incident electron energy in rydbergs.

The procedure used to calculate the resonance contribution to the excitation rate coefficient is given by Cowan.[21] The method is based on a separation of the total scattering amplitude into resonant and nonresonant parts using a projection operator formalism. The interference between the two parts is neglected and the resonance contribution is calculated in the isolated resonance approximation using single-channel distorted waves to evaluate the matrix elements which represent the coupling between the discrete resonances and the background, or direct, scattering channels. Radiative decay of the autoionizing states to singly excited states are included (up to second order in the electron-photon coupling) in the electric dipole approximation. Higher-order effects which arise from radiative transitions among autoionizing states are ignored. Such radiative cascade processes were found to have only a small effect on the resonance contributions to the electron impact excitation rates for heliumlike ions.[22]

The rate coefficient C_{id}^{cap}, for capture of a free electron can be obtained from the inverse, Auger, process by detailed balance:

$$C_{id}^{cap} = (2g_i)^{-1} \left[\frac{4\pi R}{kT} \right]^{3/2} a_0^3 \exp(-E_{di}/kT) g_d A_{di}^a \ . \quad (5)$$

Here i represents the initial state of the F-like ion and d represents the doubly excited Ne-like state formed in the capture process. g_i and g_d are the statistical weights of the states i and d, respectively, and R is the rydberg energy. A_{di}^a and E_{di} are the autoionization rate and excitation energy for the transition d to i.

The branching ratio B_{dj}^a for autoionization from the doubly excited state d of the Ne-like ion to some final (excited) state j of the F-like ion is given by

$$B_{dj}^a = \frac{A_{dj}^a}{\Gamma_a(d) + \Gamma_r(d)} \ , \quad (6)$$

where

$$\Gamma_a(d) = \sum_m A_{dm}^a, \quad \Gamma_r(d) = \sum_n A_{dn}^r \ . \quad (7)$$

In Eq. (7), m represents any of the possible final states of the F-like ion accessible by Auger decay of the doubly excited state d, n represents any of the possible states of the Ne-like ion accessible by radiative decay of the same state, and A_{dn}^r is the radiative rate for the transition $d \rightarrow n$.

The total resonance contribution to the excitation rate from state i to state f of the F-like ion is obtained by multiplying C_{id}^{cap} by B_{dj}^a and summing over all intermediate states d,

$$C_{ij}^{res} = \sum_d C_{id}^{cap} B_{dj}^a \ . \quad (8)$$

In the present work, the detailed Auger and radiative rates and the energies of the autoionizing states were calculated using the multiconfiguration Dirac-Fock model (MCDF).[23,24] The energy levels and wave functions for the $2s^2 2p^4 3lnl'$, $2s 2p^5 3lnl'$, and $2p^6 3lnl'$ $(n=3-6)$ states were calculated explicitly in intermediate coupling, including configuration interaction within the same complex by using the MCDF model in the average-level scheme (AL).[24] Separate MCDF-AL calculations were performed for the F-like configurations $1s^2 2s^r 2p^t$ where $r+t=7$, and for the singly excited Ne-like configurations $1s^2 2s^r 2p^t nl$ where $r+t=7$ and $n=3-6$.

The above-described method for treating the resonance contributions to electron impact excitation rates is well suited for highly charged positive ions with an atomic number greater than, say, 20–30, where relativistic effects and the radiative decay channels become important. Although direct scattering methods such as the close-coupling approximation properly account for the

TABLE I. Transition energies (in eV) for fluorinelike ions.

	$_{26}$Fe	$_{34}$Se	$_{42}$Mo	$_{47}$Ag	$_{54}$Xe	$_{63}$Eu
ΔE_{12}[a]	12.56	43.60	109.72	180.79	335.04	667.87
ΔE_{13}	134.14	212.54	331.18	436.26	641.22	1045.89
ΔE_{23}	121.58	168.94	221.46	255.46	306.18	378.02

[a]ΔE_{12}, ΔE_{13}, and ΔE_{23} correspond to transitions given in Eqs. (1a), (1b), and (1c), respectively.

interference between the resonant and nonresonant contributions to the scattering amplitude, currently available computer packages[1] are limited to the use of nonrelativistic target orbitals and do not explicitly include the radiative decay of the doubly excited states. However, radiative damping of the resonance contributions can be computed *a posteriori*, in some cases, using quantum-defect theory.[25]

III. RESULTS AND DISCUSSION

Table I gives the calculated energies for the $n=2$ to $n=2$ transitions in the six fluorinelike ions considered in this work. The $(2s^2 2p_{1/2} 2p^4_{3/2})^2 P_{1/2}$ states lie relatively close to the $(2s^2 2p^2_{1/2} 2p^3_{3/2})^2 P_{3/2}$ ground states and the energies of these electric quadrupole transitions [Eq. (1a)] are small compared to the transition energies for

TABLE II. Direct electron impact excitation rate coefficients and resonance contributions in cm^3/sec. Numbers in square brackets denote power of 10.

	$Z=26$		$Z=34$		$Z=42$	
Electron temp. (eV)	Direct	Resonance contributions	Direct	Resonance contribution	Direct	Resonance contribution
			$2s^2 2p^2_{1/2} 2p^3_{3/2} + e \rightarrow 2s^2 2p_{1/2} 2p^4_{3/2} + e$			
100	6.95[−11]	1.29[−11]	2.71[−11]	7.45[−13]	8.57[−12]	1.94[−14]
500	3.34[−11]	3.29[−11]	1.64[−11]	1.31[−11]	8.72[−12]	4.06[−12]
1000	2.38[−11]	1.87[−11]	1.19[−11]	1.01[−11]	6.65[−12]	4.43[−12]
1500	1.94[−11]	1.20[−11]	9.81[−12]	7.27[−12]	5.54[−12]	3.61[−12]
2000	1.68[−11]	8.45[−12]	8.53[−12]	5.44[−12]	4.84[−12]	2.89[−12]
2500	1.51[−11]	6.36[−12]	7.65[−12]	4.24[−12]	4.35[−12]	2.35[−12]
3000	1.38[−11]	5.00[−12]	6.99[−12]	3.41[−12]	3.98[−12]	1.95[−12]
4000	1.19[−11]	3.38[−12]	6.07[−12]	2.38[−12]	3.46[−12]	1.41[−12]
6000	9.74[−12]	1.92[−12]	4.96[−12]	1.39[−12]	2.83[−12]	8.56[−13]
			$2s^2 2p^2_{1/2} 2p^3_{3/2} + e \rightarrow 2s 2p^2_{1/2} 2p^4_{3/2} + e$			
100	1.53[−10]	1.43[−12]	3.89[−11]	8.55[−14]	7.45[−12]	2.28[−15]
500	2.44[−10]	6.93[−12]	1.08[−10]	3.74[−12]	5.14[−11]	1.48[−12]
1000	2.16[−10]	4.29[−12]	1.01[−10]	3.23[−12]	5.46[−11]	1.87[−12]
1500	1.92[−10]	2.83[−12]	9.17[−11]	2.40[−12]	5.18[−11]	1.60[−12]
2000	1.73[−10]	2.02[−12]	8.38[−11]	1.83[−12]	4.85[−11]	1.31[−12]
2500	1.58[−10]	1.54[−12]	7.74[−11]	1.44[−12]	4.55[−11]	1.01[−12]
3000	1.47[−10]	1.21[−12]	7.22[−11]	1.17[−12]	4.29[−11]	9.03[−13]
4000	1.30[−10]	8.28[−13]	6.43[−11]	8.23[−13]	3.87[−11]	6.62[−13]
6000	1.07[−10]	4.74[−13]	5.40[−11]	4.86[−13]	3.30[−11]	4.07[−13]
			$2s^2 2p_{1/2} 2p^4_{3/2} + e \rightarrow 2s 2p^2_{1/2} 2p^4_{3/2} + e$			
100	1.71[−10]	2.06[−12]	6.12[−11]	1.53[−13]	2.31[−11]	7.20[−15]
500	2.30[−10]	9.06[−12]	1.16[−10]	5.43[−12]	6.56[−11]	2.72[−12]
1000	2.01[−10]	5.52[−12]	1.03[−10]	4.56[−12]	6.11[−11]	3.16[−12]
1500	1.79[−10]	3.62[−12]	9.22[−11]	3.36[−12]	5.54[−11]	2.62[−12]
2000	1.62[−10]	2.58[−12]	8.38[−11]	2.55[−12]	5.08[−11]	2.11[−12]
2500	1.49[−10]	1.95[−12]	7.72[−11]	2.00[−12]	4.71[−11]	1.72[−12]
3000	1.39[−10]	1.54[−12]	7.19[−11]	1.62[−12]	4.40[−11]	1.43[−12]
4000	1.24[−10]	1.05[−12]	6.39[−11]	1.14[−12]	3.94[−11]	1.04[−12]
6000	1.04[−10]	6.00[−13]	5.36[−11]	6.70[−12]	3.32[−11]	6.34[−13]

TABLE III. Direct electron impact excitation rate coefficients and resonance contributions in cm^2/sec. Numbers in square brackets denote power of 10.

Electron temp. (eV)	$Z=47$ Direct	$Z=47$ Resonance contribution	$Z=54$ Direct	$Z=54$ Resonance contribution	$Z=63$ Direct	$Z=63$ Resonance contribution
			$2s^2 2p_{1/2}^2 2p_{3/2}^3 + e \rightarrow 2s^2 2p_{1/2} 2p_{3/2}^4 + e$			
100	3.24[−12]	1.25[−15]	5.01[−13]	2.90[−17]	1.25[−14]	8.40[−20]
500	5.86[−12]	1.76[−12]	3.14[−12]	5.81[−13]	1.13[−12]	8.06[−14]
1000	4.76[−12]	2.47[−12]	2.99[−12]	1.24[−12]	1.51[−12]	3.34[−13]
1500	4.03[−12]	2.21[−12]	2.65[−12]	1.30[−12]	1.50[−12]	4.40[−13]
2000	3.54[−12]	1.86[−12]	2.37[−12]	1.19[−12]	1.42[−12]	4.55[−13]
2500	3.19[−12]	1.56[−12]	2.16[−12]	1.05[−12]	1.33[−12]	4.35[−13]
3000	2.92[−12]	1.32[−12]	1.99[−12]	9.27[−13]	1.25[−12]	4.04[−13]
4000	2.55[−12]	9.86[−13]	1.74[−12]	7.24[−13]	1.11[−12]	3.39[−13]
6000	2.09[−12]	6.16[−13]	1.43[−12]	4.76[−13]	9.27[−13]	2.40[−13]
			$2s^2 2p_{1/2}^2 2p_{3/2}^3 + e \rightarrow 2s 2p_{1/2}^2 2p_{3/2}^4 + e$			
100	2.02[−12]	1.67[−16]	1.88[−13]	3.48[−18]	2.24[−15]	4.37[−20]
500	3.16[−11]	7.16[−13]	1.48[−11]	2.08[−13]	4.45[−12]	3.11[−14]
1000	3.77[−11]	1.18[−12]	2.12[−11]	5.50[−13]	9.30[−12]	1.66[−13]
1500	3.82[−11]	1.11[−12]	2.27[−11]	6.17[−13]	1.12[−11]	2.35[−13]
2000	3.74[−11]	9.53[−13]	2.30[−11]	5.85[−13]	1.20[−11]	2.52[−13]
2500	3.63[−11]	8.10[−13]	2.28[−11]	5.29[−13]	1.24[−11]	2.45[−13]
3000	3.51[−11]	6.93[−13]	2.25[−11]	4.72[−13]	1.25[−11]	2.30[−13]
4000	3.29[−11]	5.21[−13]	2.16[−11]	3.75[−13]	1.24[−11]	1.95[−13]
6000	2.93[−11]	3.30[−13]	1.95[−11]	2.51[−13]	1.19[−11]	1.40[−13]
			$2s^2 2p_{1/2} 2p_{3/2}^4 + e \rightarrow 2s 2p_{1/2}^2 2p_{3/2}^4 + e$			
100	1.29[−11]	6.18[−16]	5.80[−12]	2.61[−17]	2.01[−12]	1.45[−18]
500	4.78[−11]	1.29[−12]	3.16[−11]	4.77[−13]	1.92[−11]	1.31[−13]
1000	4.59[−11]	1.96[−12]	3.17[−11]	1.06[−12]	2.04[−11]	4.42[−13]
1500	4.20[−11]	1.79[−12]	2.94[−11]	1.11[−12]	1.94[−11]	5.56[−13]
2000	3.87[−11]	1.52[−12]	2.73[−11]	1.01[−12]	1.82[−11]	5.63[−13]
2500	3.60[−11]	1.29[−12]	2.55[−11]	8.94[−13]	1.71[−11]	5.32[−13]
3000	3.37[−11]	1.09[−12]	2.40[−11]	8.84[−13]	1.62[−11]	4.89[−13]
4000	3.02[−11]	8.17[−13]	2.16[−11]	6.10[−13]	1.47[−11]	4.06[−13]
6000	2.56[−11]	5.13[−13]	1.84[−11]	3.99[−13]	1.23[−11]	2.84[−13]

the dipole-allowed transitions in the ions with low atomic number. However, the $^2P_{3/2}$-$^2P_{1/2}$ fine-structure splitting increases faster with Z than does the energy of the $^2S_{1/2}$ state. As a result, the energy of the quadrupole transition exceeds the energy of the dipole-allowed transition connecting the first two excited states in the ions with higher atomic number.

The direct collisional excitation rate coefficients and the resonance contributions for six fluorinelike ions are presented in Tables II and III. In general, the resonance contribution diminishes with increasing atomic number. This can be also seen in Figs. 1(a)–1(c) where we compare the resonance contributions for several ions. The indirect collision rates initially rise and after reaching a peak they gradually diminish with increasing electron temperature. The maximum resonance contribution occurs near 500 eV for the lower Z ions, but the peak shifts slightly to higher temperatures for the more highly charged ions. Figure 2 shows the direct excitation rate coefficients for the electric quadrupole transition as a function of electron temperature. The direct rates also diminish with increasing ionic charge for all three transitions.[19]

For $26 \leq Z \leq 63$, the direct rate coefficient for the dipole-forbidden, i.e., electric quadrupole, transition is much smaller than those for the dipole-allowed transitions, while the resonance contribution is the greatest for the former. Hence, the resonance enhancement is most significant for the dipole-forbidden $^2P_{3/2}$-$^2P_{1/2}$ transition. This is consistent with results reported by Pradhan *et al.*,[2] who noted the same trend for helium-like ions. In Fig. 3 we compare the direct and the total (direct plus resonant) rate coefficients for all three transitions in Fe^{17+}. For the two dipole-allowed transitions the total rates are only slightly greater than the direct rates while the resonance contribution increases the excitation rate by a factor of 2, near 500 eV, for the dipole-forbidden transition. In all cases the resonance enhancement decreases at high electron temperatures.

In Figs. 4 and 5 we show similar comparisons for Mo^{33+} and Eu^{54+}, respectively. Again, the resonance contribution to the excitation rates is important only for

the dipole-forbidden, $^2P_{3/2}$-$^2P_{1/2}$ transition. Comparing Figs. 3(a), 4(a), and 5(a), it can be seen that the resonance enhancement decreases with increasing ionic charge. This is due to the fact that the radiative rates increase approximately as Z^4 and the radiative channels

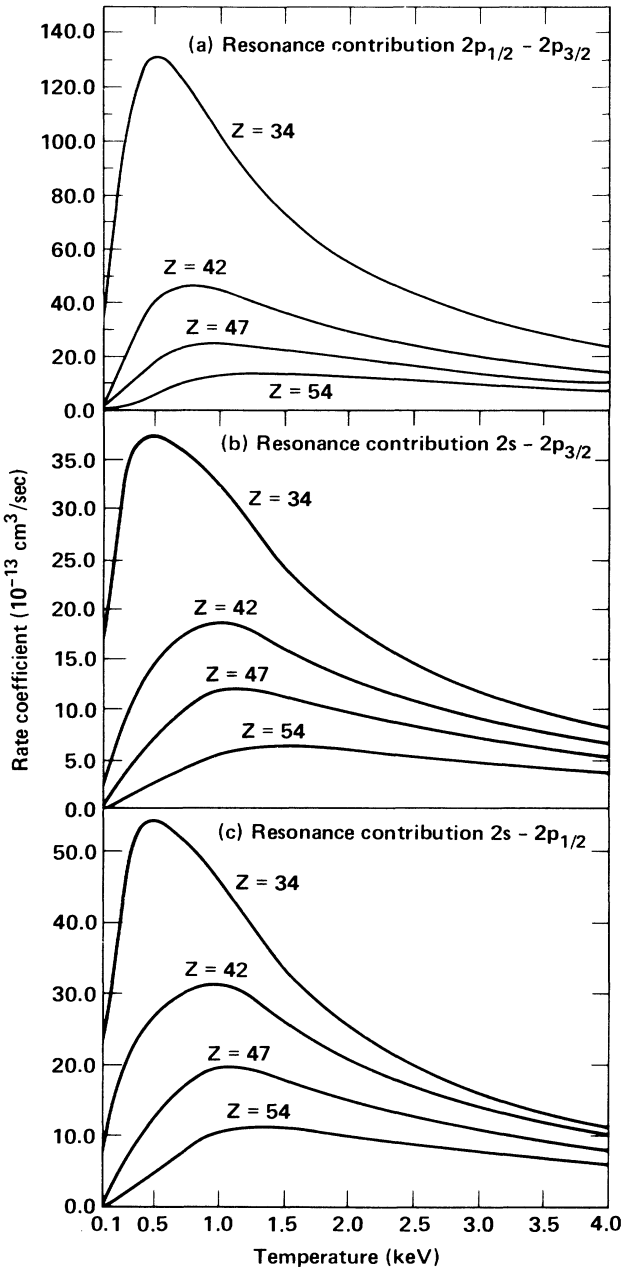

FIG. 1. (a) Resonance contribution to the excitation rate coefficients for the $2s^2 2p_{1/2}^2 2p_{3/2}^3 \rightarrow 2s^2 2p_{1/2} 2p_{3/2}^4$ transition in fluorinelike ions. (b) Same as (a), but for the $2s^2 2p_{1/2}^2 2p_{3/2}^3 \rightarrow 2s 2p_{1/2}^2 2p_{3/2}^4$ transition. (c) Same as (a), but for the $2s^2 2p_{1/2} 2p_{3/2}^4 \rightarrow 2s 2p_{1/2}^2 2p_{3/2}^4$ transition.

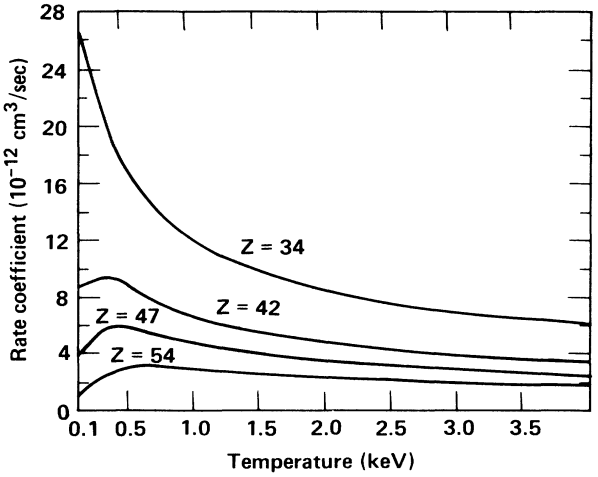

FIG. 2. Rate coefficients for the direct electron impact excitation of the $2s^2 2p_{1/2}^2 2p_{3/2}^3 \rightarrow 2s^2 2p_{1/2} 2p_{3/2}^4$ transition in fluorinelike ions.

become the dominant decay mode for the doubly excited states in the heavier ions. To illustrate this further, we show in Fig. 6 the average L-shell fluorescence yield as a function of atomic number for the $3l3l'$ doubly excited states of Ne-like ions. Here the average fluorescence yield $\bar{\omega}$ is defined as

$$\bar{\omega} = \frac{\bar{A}_r}{\bar{A}_r + \bar{A}_a} , \tag{9}$$

where $\bar{A}_r$ and $\bar{A}_a$ are the statistically weighted averages of the detailed radiative and Auger rates, respectively. Figure 6 clearly shows that $\bar{\omega}$ increases rapidly with increasing atomic number. Thus, for the heavier ions, the radiative channel leading to dielectronic recombination is dominant, and the resonance contributions to the excitation rates are less significant.

The major contributions to the resonance enhancement arise from electron capture into doubly excited states having low principal quantum numbers. This is to be expected since the Auger rates vary approximately as n^{-3} and the resonance enhancement scales as n^{-6} [See Eqs. (5), (6), and (8)]. In Fig. 7 we show the resonance contribution as a function of principal quantum number for the $^2p_{3/2}$-$^2p_{1/2}$ transition in Mo^{33+}. At lower electron temperatures the resonance contribution is concentrated in the $3l3l'$ intermediate states and drops sharply for the $3lnl'$ states with $n \geq 4$. At higher electron temperatures, the largest contribution is still from the $3l3l'$ states, but the contribution from the higher n states is no longer negligible. With the total excitation rates reported here, we include contributions from the $3lnl'$ doubly excited states with $3 \leq n \leq 6$. Finally, it should be noted that loosely bound doubly excited states with high n may be destroyed by collisions in a very dense plasma. But

the lower-lying doubly excited levels which have the largest effect on the collisional excitation rates for highly charged ions are less likely to suffer from density effects.

IV. CONCLUSIONS

We have studied the effects of autoionizing resonances on the rates for electron collisional excitation of the $n=2$ to $n=2$ transitions in fluorinelike ions. We found that the contributions from doubly excited resonances significantly increase the rate coefficients for the electric-dipole-forbidden (electric-quadrupole-allowed) $2s^2 2p_{1/2}^2 2p_{3/2}^3 \rightarrow 2s^2 2p_{1/2} 2p_{3/2}^4$ transition. The largest resonance enhancement, about a factor of 2, occurs in low-Z ions, such as Fe^{17+} (near $T=0.5$ keV) and Se^{25+}

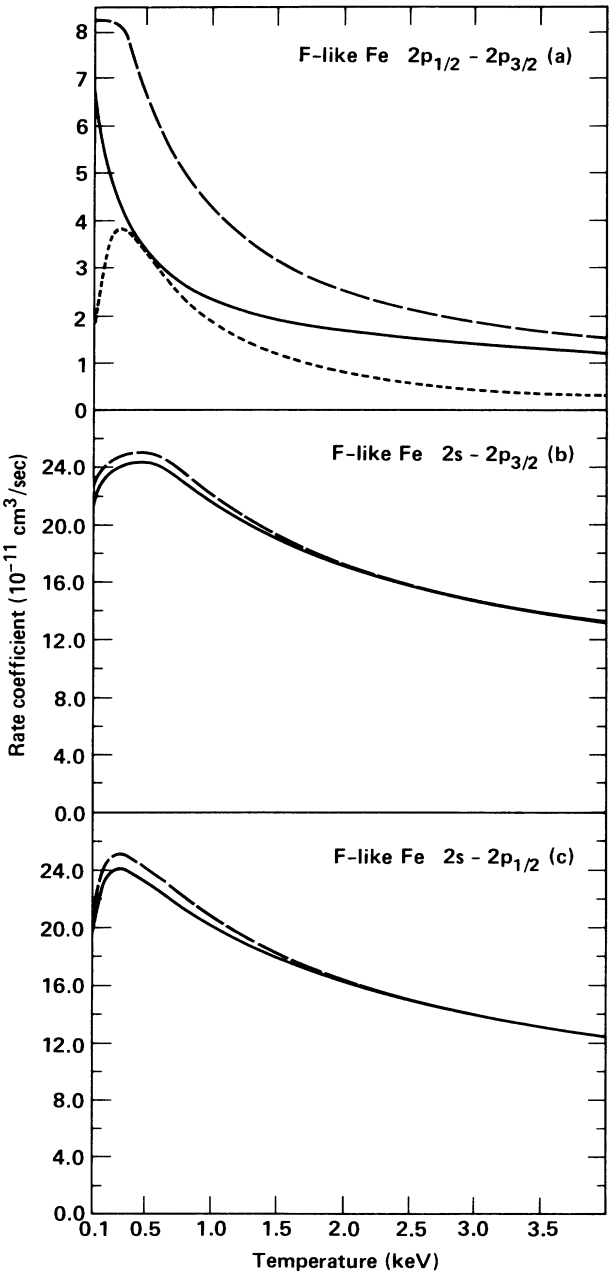

FIG. 3. Excitation rate coefficients for Fe^{17+}; — — —, total; ——, direct contribution; · · · ·, resonance contribution.

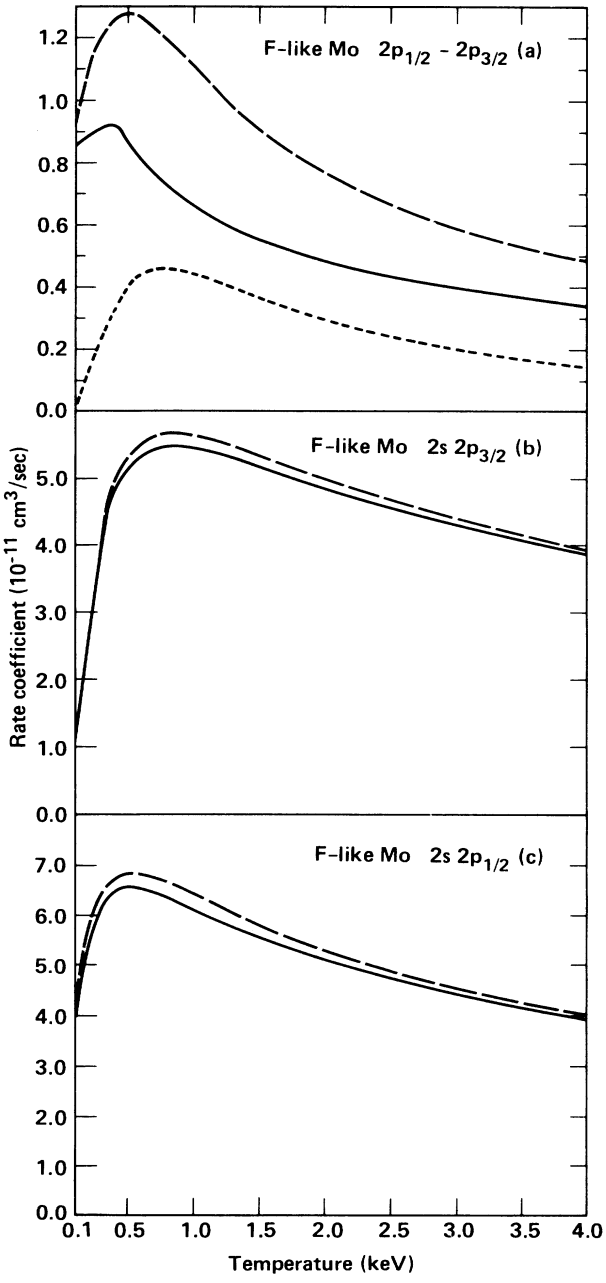

FIG. 4. The same as Fig. 3 except for Mo^{33+}.

(near $T=1.0$ keV). The resonance effects become less significant for the higher-Z ions because of the increasing dominance of the radiative channels. For each ion, the resonance enhancement diminishes at higher electron temperatures and it is always quite small for the two dipole-allowed transitions.

Based on the present results obtained for fluorinelike ions, we expect that autoionizing resonances will have a

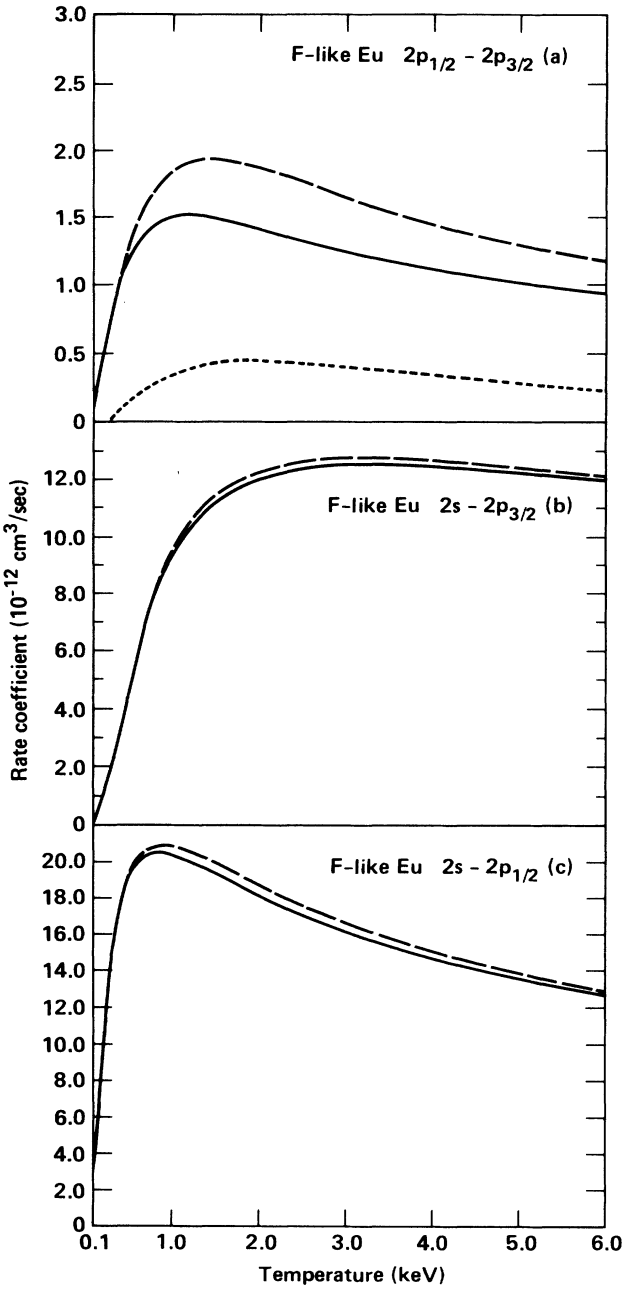

FIG. 5. The same as Fig. 3 except for Eu^{54+}.

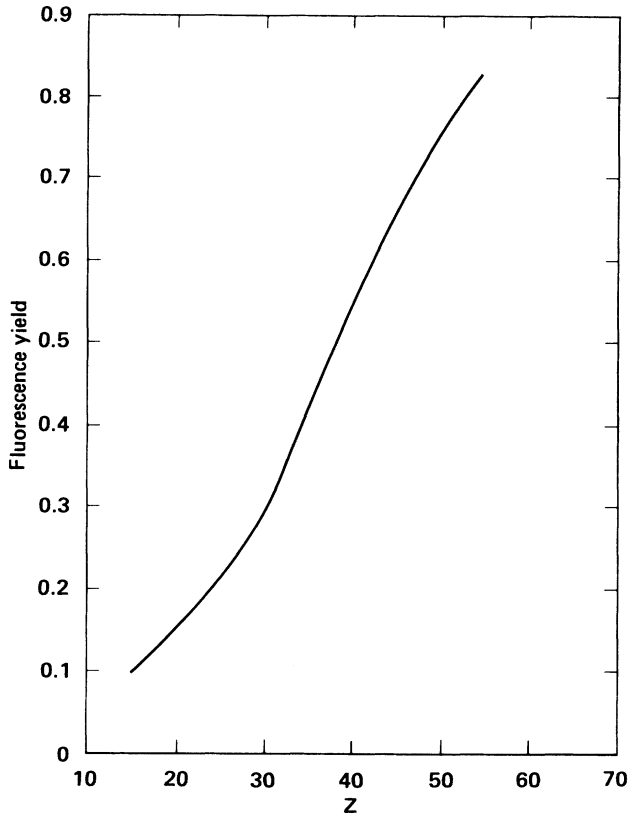

FIG. 6. Average L-shell fluorescence yield of the $3l3l'$ doubly excited states of neonlike ions as function of atomic number.

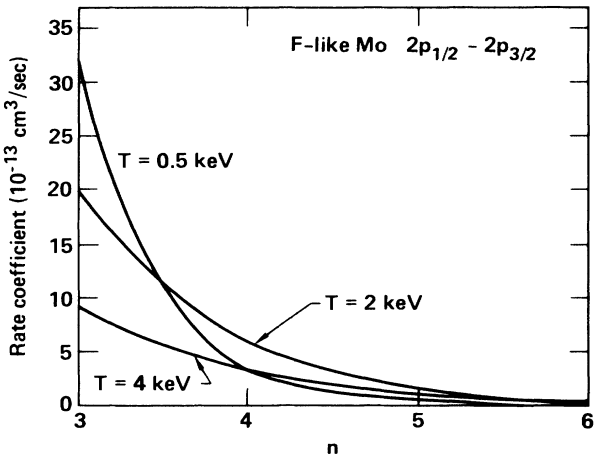

FIG. 7. Contributions from the $3lnl'$ intermediate states to the excitation rate coefficient of the $^2p_{3/2}$-$^2p_{1/2}$ transition in Mo^{33+} as function of principal quantum number n.

similar effect on the electron impact excitation rates of $n=2$ to $n=2$ transitions in other isoelectronic sequences with partially filled L shells, e.g., oxygenlike nitrogenlike, etc. Indeed, in calculations currently underway for oxygenlike selenium[26] we are finding substantial resonance enhancements for the electric-dipole-forbidden transitions. The results of these calculations[26] will be reported in due course.

ACKNOWLEDGMENT

Work was performed under the auspices of the U. S. Department of Energy by Lawrence Livermore National Laboratory under Contract No. W-7405-Eng-48.

[1]For a recent review of calculations on electron impact excitation of positive ions, see R. J. W. Henry, Phys. Rep. **68**, 1 (1981).

[2]A. K. Pradhan, D. W. Norcross, and D. G. Hummer, Phys. Rev. A **23**, 619 (1981); Astrophys. J. **246**, 1031 (1981); A. K. Pradhan, Phys. Rev. A **28**, 2113 (1983).

[3]K. Bhadra and R. J. W. Henry, Phys. Rev. A **26**, 1848 (1982).

[4]R. E. H. Clark, A. L. Merts, J. B. Mann, and L. A. Collins, Phys. Rev. A **27**, 1812 (1983).

[5]K. J. Reed and A. Hazi, in Proceedings and Abstracts of the Eighth International Conference on Atomic Physics, Göteborg, 1982, edited by I. Lindgren, A. Rosén, and S. Svanberg, p. 76 (unpublished).

[6]M. S. Pindzola, D. C. Griffin, and C. Bottcher, Phys. Rev. A **32**, 822 (1985).

[7]U. Feldman and G. A. Doschek, J. Opt. Soc. Am. **67**, 726 (1977).

[8]J. F. Seely, T. W. Phillips, R. S. Walling, J. Bailey, R. E. Stewart, and J. H. Scofield, Phys. Rev. A **34**, 2924 (1986).

[9]M. D. Rosen, *et al.*, Phys. Rev. Lett. **54**, 106 (1985); D. L. Matthews, *et al.*, Phys. Rev. Lett. **54**, 110 (1985).

[10]B. J. MacGowan *et al.*, J. Appl. Phys. (to be published).

[11]M. H. Chen, Phys. Rev. A **34**, 1079 (1986).

[12]B. L. Whitten, A. U. Hazi, M. H. Chen, and P. L. Hagelstein, Phys. Rev. A **33**, 2171 (1986).

[13]P. L. Hagelstein, M. D. Rosen, and V. L. Jacobs, Phys. Rev. A **34**, 1931 (1986).

[14]P. L. Hagelstein, Phys. Rev. A **34**, 924 (1986).

[15]A. L. Merts, J. B. Mann, W. D. Robb, and N. H. Magee, Los Alamos National Laboratory Report No. LA-8267-MS, 1980 (unpublished).

[16]J. Davis, P. C. Kepple, and M. Blaha, J. Quant. Spectrosc. Radiat. Transfer **16**, 1043 (1976).

[17]A. K. Bhatia and U. Feldman, J. Appl. Phys. **53**, 4711 (1982).

[18]A. K. Bhatia, U. Feldman, and G. A. Doschek, J. Appl. Phys. **51**, 1464 (1980).

[19]K. J. Reed (unpublished).

[20]P. L. Hagelstein, Phys. Rev. A **34**, 874 (1986); also P. L. Hagelstein and R. K. Jung, presented at the Third International Conference/Workshop on the Radiative Properties of Hot Dense Matter, Williamsburg, VA, 1985 (unpublished).

[21]R. D. Cowan, J. Phys. B **13**, 1471 (1980).

[22]H. Zhang and D. H. Sampson, Astrophys. J. Suppl. Ser. **63**, 487 (1987), and private communication.

[23]I. P. Grant *et al.*, Comput. Phys. Commun. **21**, 207 (1980).

[24]M. H. Chen, Phys. Rev. A **31**, 1499 (1985).

[25]A. K. Pradhan, Phys. Rev. Lett. **47**, 79 (1981).

[26]K. Reed and M. Chen (unpublished).